

## DISTURBANCES IN AN ACCELERATED BOUNDARY LAYER UNDER INFLUENCE OF MODERATE FREE-STREAM TURBULENCE

**Dmitry S. Sboev\***

**\* Central aerohydrodynamic institute n.a. Prof. N.E. Zhukovsky (TsAGI),  
Zhukovsky, Russia**

**Keywords:** *freestream non-uniformities, longitudinal streaks, vorticity stretching*

### Abstract

*An experimental investigation of a perturbed laminar boundary layer on the flat plate at negative incidence is presented. Both stationary and nonstationary free stream disturbances were introduced in a flow by means of a turbulizing grid. It was found that inside a boundary layer the two types of disturbed motions are developing. The stationary longitudinal structures were produced by small non-uniformities of incoming flow. In comparison, this effect was relatively weak in a near zero pressure gradient boundary layer on the same model at similar upstream conditions. Low frequency velocity fluctuations interacts with these structures, so the entire flow field becomes increasingly three-dimensional.*

### 1 Introduction

Accelerated boundary layers under influence of free stream turbulence (FST) are important in many applications. The common experimental practice to investigate their properties is to place a model at some distance behind a turbulence-generating grid. It is well known that the mean flow behind grid could be disturbed in transverse directions. These mean-flow non-uniformities becomes rather small at the distances about 20-40 grid mesh sizes. However, they are not disappearing at all even after much longer development. By means of some receptivity mechanisms [1, 2] such non-uniformities could lead to a spanwise modulation of a nominally two-dimensional boundary layer and affect the development of

non-stationary disturbances induced by FTS. The present experimental results indicate that this effect could be more pronounced in an accelerated boundary layer in comparison to the boundary layer that develops on the same model with a near-zero pressure gradient.

### 2 Experimental set-up

The sketch of an experimental set-up is shown in the Fig. 1. The elevated FST level about 1.4% was generated by means of a grid installed upstream the model at the distance of 175 mesh size. The grid was woven from the 0.4 mm wire and had mesh size 2 mm. The free stream velocity  $U_{ref}$  was 9.9 m/sec. The model used

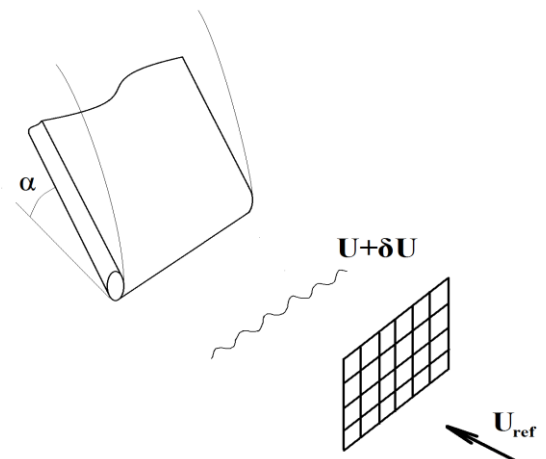


Fig. 1. Experimental set-up.

was a blunt nosed 12 mm thick flat plate with the chord  $C = 200$  mm. The hot-wire surveys were performed in a boundary layer as well as in the free stream. The coordinate system used

had the longitudinal axis  $X$ , spanwise  $Z$  and normal  $Y$  respectively. The origin was located at the leading edge.

The plate was installed at the incidence  $\alpha = -30^\circ$  or  $0$  in the test section of a low turbulence wind tunnel, so the experimental data were obtained in an accelerated boundary layers. At  $\alpha = -30^\circ$  the Hartree parameter was almost constant throughout the measurement region ( $0 < X/C < 0.8$ ) and equal about 0.45. The distributions of the edge velocity  $U_e$  is shown in the Fig. 2. In the undisturbed case the  $U_e$  is very close to the power law, while with the grid installed the agreement is somewhat worse.

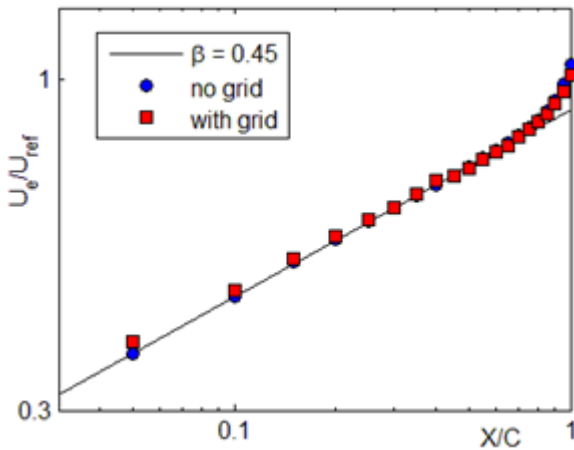


Fig. 2. The edge velocity distributions,  $\alpha = -30^\circ$ ,  $Y = 10$  mm.

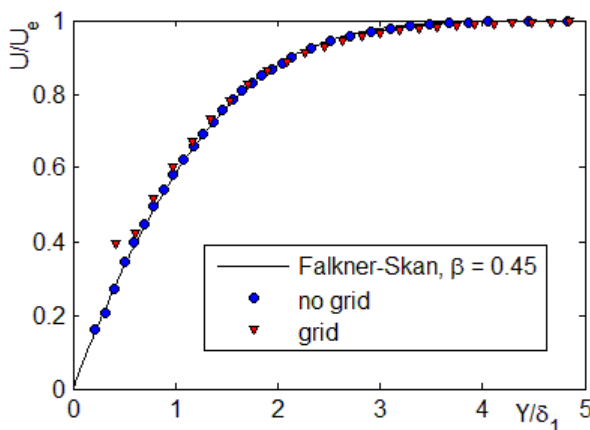


Fig. 3. The mean velocity profiles in the boundary layer,  $X/C = 0.575$ ,  $\alpha = -30^\circ$ .

Also, the mean velocity profiles in the undisturbed boundary layer are in excellent agreement with the Falkner-Skan solution for

$\beta = 0.45$  (see Fig. 3). The spanwise averaged profile obtained in the elevated FST case again slightly differs from the theoretical one. The excess of velocity near the wall and defect in the upper half of the boundary layer are visible. At zero incidence, due to the thick leading edge and slight acceleration of the flow, the boundary layer relaxes to the Blasius one only at  $X/C = 0.575$  ( $X = 115$  mm).

### 3 The stationary non-uniformities of incoming flow

The measurements for the detection of spatial mean flow non-uniformities usually suffers from a low-frequency temporal variations of the flow. To overcome this the correlation measurements are needed. The method used here was originally proposed in [1].

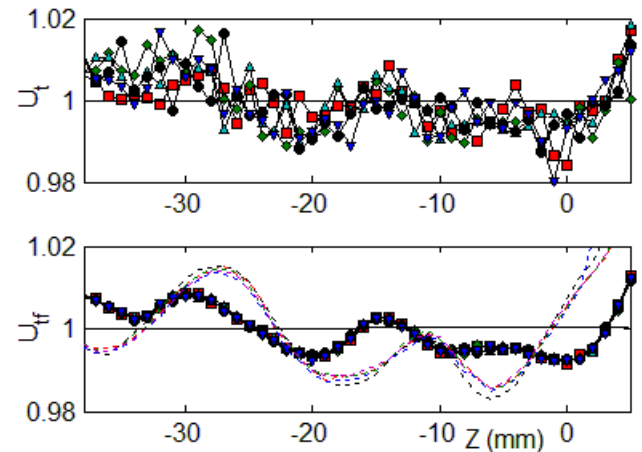


Fig. 4. The five realisations of spanwise distributions of  $U_t$  at the distance 120 mm upstream the model (upper plot) and five realisations of  $U_t/U_{ref}$  at the 120 (symbols) and 30 mm (dashed lines) upstream the model (lower plot),  $\alpha = -30^\circ$ .

Denote as  $U_{trav}$  the velocity that measured by the hot-wire and averaged during period  $T$ . The  $\bar{U}_{trav}$  is the spanwise averaging of  $U_{trav}$ . As it shown in Fig. 4 the spanwise distribution of the  $U_t = U_{trav}/\bar{U}_{trav}$  exhibits the considerable scattering. As the velocity  $U_{ref}$  had been measured by the Pitot-static tube at fixed position during the same period  $T$ , it is convenient to introduce the ensemble-averaged

velocity  $U_{fix}$  as mean value of  $U_{ref}$  during the measurements of the  $U_{irav}$  distributions and  $U_f$  as  $U_{ref}/U_{fix}$ . The ratio  $U_{if} = U_i/U_f$  could be used as measure of spanwise mean flow non-uniformities produced by the grid.

As it seen from the Fig. 4, the procedure described allows to reveal the regular spanwise variations in the incoming flow with the dominant wavelength about 10-12 mm and amplitude  $\delta U$  order  $0.001U_{ref}$ . It is also important that, as the flow develops from the -120 to -30 mm, the value of  $\delta U$  becomes approximately two times larger. This observation is in qualitative agreement with the vorticity stretching theory [3] that predicts the amplification of the  $Y$ -component of the vorticity on curved potential flow streamlines.

#### 4 The boundary layer disturbances

The measurements of  $U(Y, Z)$  distributions inside the boundary layer were performed at five streamwise positions. The example of mean velocity at  $X/C = 0.575$ ,  $\alpha = -30^\circ$  is given in Fig. 5. It demonstrates the periodic spanwise deformation of the mean flow under the action of the steady disturbances. The mean flow field of  $\Delta U$ , which is the  $U(Y, Z)$  field with the spanwise-averaged profile removed, is shown in Fig. 6. The alternating regions of the velocity excesses and defects in the spanwise direction are clearly visible. As the normal coordinate normalized with the value of spanwise-averaged boundary layer thickness  $\delta$ , the Fig. 5 and 6 shows that the most pronounced distortions are contained well inside the boundary layer and decays outside of it. These data indicates that a system of stationary longitudinal structures arises in the boundary layer. Their development leads to the spanwise variations of the local boundary layer thickness.

The spanwise wavenumber spectrum of  $\Delta U$  is shown in Fig. 7. The single maximum of the spectrum is located at  $Y/\delta = 0.4-0.45$ ,  $\beta/2\pi = 0.091 \text{ mm}^{-1}$  and coincides very well to the dominant wavelength in the free stream. The value of the dominant wavelength inside the boundary layer approximately corresponds to five local thickness of the undisturbed boundary

layer. The wall-normal profile of steady disturbance  $\Delta U_\beta$  is plotted in Fig. 8. It has a bell-like shape with single maximum located at the middle of the boundary layer and similar to the profiles of the low-frequency unsteady Klebanoff modes in zero pressure gradient boundary layers.

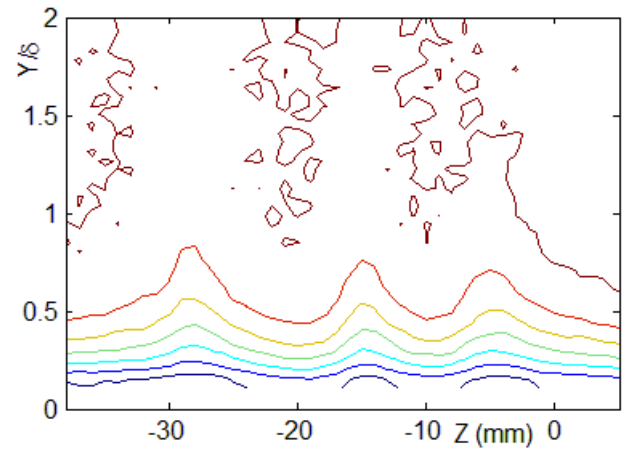


Fig. 5. The mean velocity field  $U(Y, Z)/U_e$  at the  $X/C = 0.575$ ,  $\alpha = -30^\circ$ . The contour step is 0.1 from the 0.3 to 0.9.

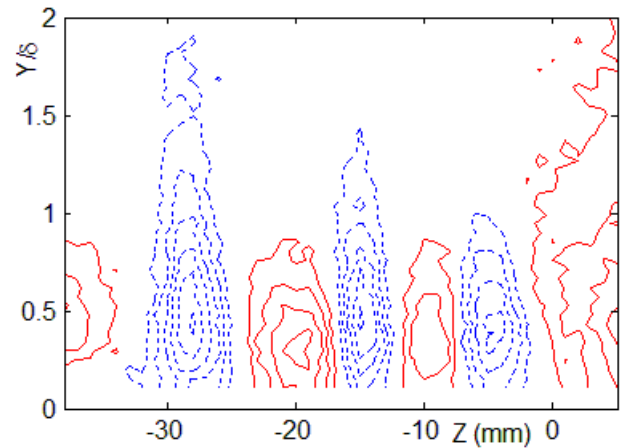


Fig. 6. The contour plot of the  $\Delta U/U_e$  field at the  $X/C = 0.575$ ,  $\alpha = -30^\circ$ . The solid and dashed contours corresponds to the positive and negative values respectively. The contour step is 0.02.

The growth of stationary disturbances with the dominant wavenumber, that corresponds to the freestream one, is shown in Fig. 9, where the streamwise distributions of  $\Delta U_\beta$  is plotted.  $\Delta U_\beta$

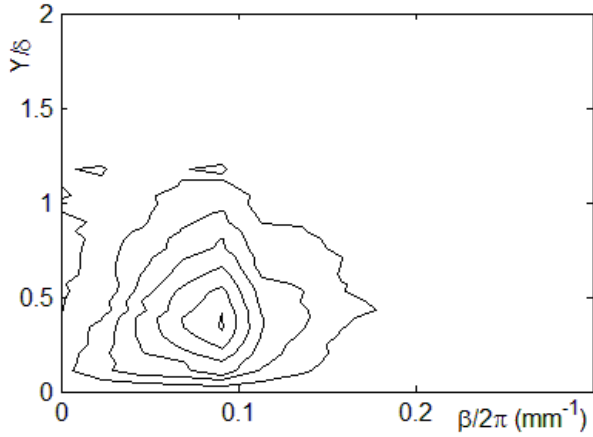


Fig. 7. The spanwise wavenumber spectrum of  $\Delta U$  at the  $X/C = 0.575$ ,  $\alpha = -30^\circ$ .

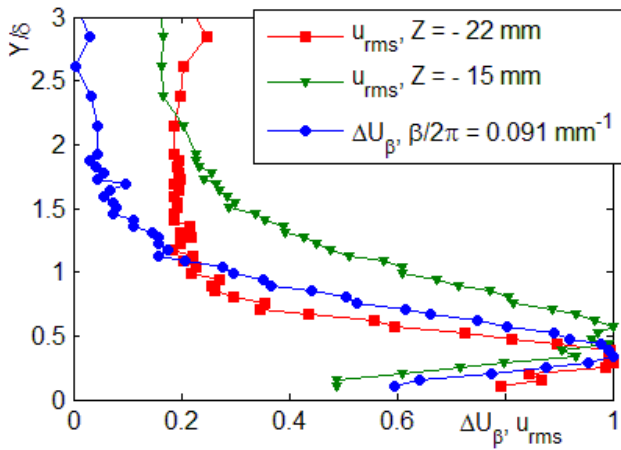


Fig. 8. The wall-normal profiles of disturbances at the  $X/C = 0.575$ ,  $\alpha = -30^\circ$ . The profiles are normalized with their maxima.

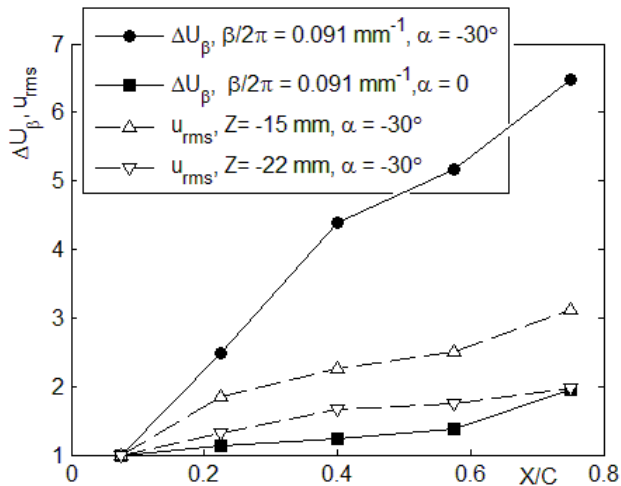


Fig. 9. The growth of stationary and traveling disturbances measured at  $Y/\delta = 0.4$

normalized with their amplitude at the first measurements station. For comparison the data obtained at zero incidence is also plotted. It is seen from this figure that growth of  $\Delta U_\beta$  is almost linear. The striking feature is that the longitudinal stationary structures in the  $\alpha = -30^\circ$  case are growing much faster than in the boundary layer with the near-zero pressure gradient. This finding confirms the results of the flow visualization experiment [2]. As it follows from the spatial transient growth theory [4] a favorable pressure gradient leads to suppression of the transient growth mechanism. Also the spanwise scale of the stationary streaks is highly suboptimal in comparison with the transient growth theory predictions that usually gives values about two local boundary layer thickness. So the question arises of mechanism that governs the formation and growth of the steady streaks in this case. It is well known [5, 6] that the stagnation flow (as well as the nonorthogonal stagnation flow) is linearly stable. The receptivity and enhanced growth in this case could be provided by means of vorticity stretching mechanism on curved streamlines, which is somewhat similar to proposed in [7] or in [8]. The above mentioned amplification of the freestream non-uniformities in a potential flow outside the boundary layer is also supports this conclusion.

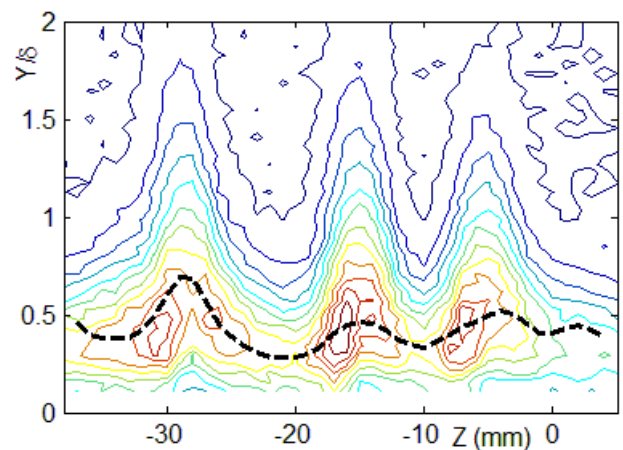


Fig. 10. Contour plot of  $u_{rms}/U_{ref}$  at  $X/C = 0.575$ ,  $\alpha = -30^\circ$ . The contour step is 0.005 from the 0.01 to 0.07. The bold dashed line shows the position of the  $\partial U/\partial Z$  maximum.

The amplitude of fluctuating velocity in the boundary layer is also modulated in spanwise direction with the same period of modulation as for the steady disturbances (see Fig. 10). The shapes of the wall-normal profiles for the traveling disturbances also had common features with the Klebanov modes (Fig. 9). However in the positions corresponding to the peaks and valleys of the  $U(Y, Z)$  field the  $u_{rms}$  profiles are shifted relatively each other. It is interesting that the wall-normal positions of the  $u_{rms}$  maxima is well correlated with the positions of maxima of spanwise gradient of the mean velocity.

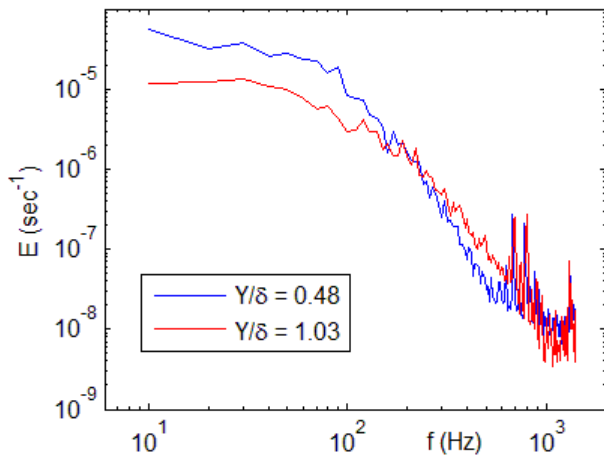


Fig. 11. The power spectral densities of velocity fluctuations in the boundary layer at  $X/C = 0.575$ ,  $Z = -15$  mm,  $\alpha = -30^\circ$ .

The spectra of traveling disturbances shows the amplification of low-frequency fluctuations inside the boundary layer that is common feature of development of the FST-induced perturbations. However, as it seen from the Fig. 11, the high-frequency components are decaying rather slow toward the wall in comparison with well-known behaviour in the zero pressure gradient case. This was observed as at the peaks as well at the valley positions.

The effect of spanwise modulation of the amplitudes of unsteady disturbances is clearly connected with the receptivity issues, because after its initial phase the growth of fluctuations only slightly depends on spanwise position at  $X/C > 0.225$  (Fig. 9). As it seen from the Fig. 9, the growth of traveling disturbances corresponds to a power law  $X^a$ ,  $a < 1$ .

## 5 Conclusions

The experiment had showed that inside an accelerated boundary layer under influence of grid generated turbulence the two types of disturbed motions are developing. The first one is the stationary streamwise velocity distortions with the spanwise wavelength equal to the free-stream wavelength. It was observed that growth of the mean flow non-uniformities in the accelerated boundary layer was much faster than in the case when the model was installed at zero angle of attack. The second type of boundary layer disturbances is well-known low-frequency fluctuations generated by FST. However their initial growth depends on the spanwise position. It leads to the spanwise modulation of the rms-amplitude of velocity fluctuations in the boundary layer.

## References

- [1] Deyhle H. *Einfluß der äußeren Stromungsbedingungen auf den Transitionsprozeß einer dreidimensionalen Grenzschicht*. Dissertation zum Dr.-Ing. an der TH Hannover, 1993.
- [2] Brylyakov A.P., Zanin B.Yu., Zharkova G.M. and Sboev D.S. Effect of Turbulizing Grid Near Wake on a Boundary Layer on a Wedge. *Proc. of ICMAR' 2002*, Pt. II, Novosibirsk (Russian Federation), pp 56-60, 2002.
- [3] Sadeh W.Z., Suter S.P. and Maeder P.F. Analysis of vorticity amplification in the flow approaching a two-dimensional stagnation point. *Zeitschrift für angewandte Mathematik und Physik*, Vol. 21, No. 5, pp 717-742, 1970.
- [4] Tumin A. and Ashpis D.E. Optimal Disturbances in Boundary Layers Subject to Streamwise Pressure Gradient. *AIAA Journal*, Vol. 41, No. 11, pp 2297-2300, 2003.
- [5] Wilson S.D.R. and Gladwell I. The stability of a two-dimensional stagnation flow to three-dimensional disturbances. *Journal of Fluid Mechanics*, Vol. 84, No. 3, pp 517-527, 1978.
- [6] Boiko A.V. and Sboev D.S. On stability of 2D non-orthogonal stagnation flow. *Thermophysics and Aeromechanics*, Vol. 10, No. 4, pp 549-553, 2003.
- [7] Suter S.P., Maeder F.P. and J. Kestin J. On the sensitivity of heat transfer in the stagnation-point boundary layer to free-stream vorticity. *Journal of Fluid Mechanics*, Vol. 16, No. 4, pp 497-520, 1963.
- [8] Wu X. and Durbin P.A. Evidence of longitudinal vortices evolved from distorted wakes in a turbine passage. *Journal of Fluid Mechanics*, Vol. 446, pp 199-228, 2001.

**Contact Author Email Address**

mailto: t124@inbox.ru

**Copyright Statement**

The authors confirm that they, and/or their company or organization, hold copyright on all of the original material included in this paper. The authors also confirm that they have obtained permission, from the copyright holder of any third party material included in this paper, to publish it as part of their paper. The authors confirm that they give permission, or have obtained permission from the copyright holder of this paper, for the publication and distribution of this paper as part of the ICAS proceedings or as individual off-prints from the proceedings.